

- Devreotes, *FASEB J.* **5**, 3078 (1991); G. P. Downey, *Curr. Opin. Immunol.* **6**, 113 (1994).
2. O. D. Weiner et al., *Nature Cell Biol.* **1**, 75 (1999).
 3. Z. Xiao et al., *J. Cell Biol.* **139**, 365 (1997).
 4. G. Servant, O. D. Weiner, E. R. Neptune, J. W. Sedat, H. R. Bourne, *Mol. Biol. Cell* **10**, 1163 (1999).
 5. C. A. Parent et al., *Cell* **95**, 81 (1998); C. A. Parent and P. N. Devreotes, *Science* **284**, 765 (1999).
 6. R. Meili et al., *EMBO J.* **18**, 2092 (1999).
 7. Culture and differentiation of HL-60 cells with 1.3% dimethyl sulfoxide (DMSO) were performed as described (4).
 8. The fusions of the PH domains of the protein kinase B (PKB/AKT) kinase and the C5aR with GFP are already described [P. Varnai and T. Balla, *J. Cell Biol.* **143**, 501 (1998)] (4). HL-60 cells were transfected by electroporation. Stable cell lines were generated with 1 mg/ml active G-418. Further details of these methods are available at (9).
 9. Supplemental material is available at www.sciencemag.org/feature/data/1044239.shl.
 10. Microscopic analysis of HL-60 cells was performed at room temperature as already described (4). For point-source stimulation, custom-made micropipets with an opening of $0.5 \pm 0.2 \mu\text{m}$ (Eppendorf Femtotips; Fisher Scientific, Pittsburgh, PA) were used. Chemoattractant was back loaded, and air bubbles were pushed out with a microinjection device. The micropipette was placed at the desired coordinates, and a chemotactic gradient was generated with passive diffusion from the tip.
 11. Seventeen different sessions of point-source stimulation were performed with PHAKT-GFP expressing HL-60 cells. In these experiments, 15 of 23 cells migrating toward the micropipette showed translocation at the leading edge. Failure to detect recruitment in a minority of the polarizing cells probably indicates a threshold phenomenon. That is, the stimulation received by individual cells exposed to the pipette is weaker than that received by cells in a uniform concentration (100 nM) of fMLP, which causes recruitment in 96% of cells [Web figure 4D (9)]. Eleven different sessions of point-source stimulation were performed with GFP-expressing HL-60 cells. In these experiments, as expected, we could not detect any increase of the fluorescent signal at the leading edge of 30 cells migrating toward the micropipette. The C5a receptor-GFP chimera (C5aR-GFP) was shown previously to behave as a spatially unbiased probe of plasma membrane concentration when expressed in a neutrophil-like cell line, PLB-985 (4). Similarly, we detected no apparent increase of C5aR-GFP fluorescence at the leading edge of HL-60 cells.
 12. To determine the apparent shape of the chemotactic gradient generated by the Femtotips, we used a fluorescent dye of molecular weight similar to fMLP (MW: 437.6): sulforhodamine 101 (MW: 606.7; Molecular Probes, Eugene, OR). Two different Femtotips were tested and similar gradients were observed. IVE software [H. Chen, D. D. Hughes, T. A. Chan, J. W. Sedat, D. A. Agard, *J. Struct. Biol.* **116**, 56 (1996)] was used to calculate fluorescence intensity along the lines indicated for the fluorescent ligand and PHAKT-GFP recruitment (Fig. 1B).
 13. Virtually all differentiated HL-60 cells showed recruitment of PHAKT-GFP to the plasma membrane [96%; Web figure 4D (9)] when exposed to a uniform increase in fMLP concentration (from 0 to 100 nM fMLP), but only ~50% of the cells polarized morphologically within the first 4 min of stimulation. Of the cells that did polarize, ~50% (that is, ~25% of the entire population) showed periods of asymmetric recruitment of PHAKT-GFP to ruffles at the cell's protruding edge.
 14. Treatment of HL-60 cells with toxins and inhibitor were as follows: latrunculin-B (Calbiochem, La Jolla, CA) was added on plated cells at a final concentration of 20 $\mu\text{g/ml}$, and cells were incubated for 5 to 10 min at room temperature. PTX (List Biological Laboratories, Campbell, CA), which acts by inhibiting signal transduction by G_i proteins, was added directly to the cell culture medium a final concentration of 1 $\mu\text{g/ml}$, and cells were incubated at 37°C for a period of 16 to 22 hours. For LY 294002 (Calbiochem, La Jolla, CA) treatment, a stock solution (100 \times) was prepared in 100% DMSO just before use. Cells plated on glass cover slips as described (4), were incubated for 20 min at room temperature with a freshly diluted solution (100 to 300 μM) of LY 294002 in modified Hank's balanced salt solution (4). *Clostridium difficile* toxin-B (TechLab, Blacksburg, VA), was added directly to the cell culture medium at a final concentration of 90 $\mu\text{g/ml}$. Cells were incubated at 37°C with the toxin for not less than 2 hours and not more than 4 hours, a period in which the best inhibition of fMLP-induced ruffling and actin polymerization responses was observed without excessive loss of cell viability. Further experimental details for treatments with LY 294002 and *C. difficile* toxin are available at (9).
 15. A. Abo et al., *Nature* **353**, 668 (1991); U. G. Knaus et al., *Science* **254**, 1512 (1991); D. Cox et al., *J. Exp. Med.* **186**, 1487 (1997); G. M. Bokoch, *Blood* **86**, 1649 (1995).
 16. Chemotaxis, F-actin generation, and superoxide production induced by chemoattractants are markedly impaired in neutrophils lacking one GTPase, Rac2 [A. W. Roberts et al., *Immunity* **10**, 183 (1999)].
 17. A. Hall, *Annu. Rev. Cell Biol.* **10**, 31 (1994); S. H. Zigmond et al., *J. Cell Biol.* **138**, 363 (1997); S. H. Zigmond et al., *J. Cell Biol.* **142**, 1001 (1998); L. Ma et al., *J. Cell Biol.* **140**, 1125 (1998); L. Ma, R. Rohatgi, M. W. Kirschner, *Proc. Natl. Acad. Sci. U.S.A.* **95**, 15362 (1998); A. Hall, *Science* **279**, 509 (1998); D. J. Mackay and A. Hall, *J. Biol. Chem.* **273**, 20685 (1998); E. Bi and S. H. Zigmond, *Curr. Biol.* **9**, R160 (1999).
 18. P. Sehr et al., *Biochemistry* **37**, 5296 (1998); I. Just et al., *Nature* **375**, 500 (1995).
 19. G. Servant et al., unpublished data.
 20. Preliminary experiments show that PHAKT-GFP-expressing HL-60 cells also migrated toward a micropipette delivering a point source of insulin. However, under these conditions we have not been able to detect translocation of PHAKT-GFP to the plasma membrane.
 21. S. R. James et al., *Biochem. J.* **315**, 709 (1996); D. Stokoe et al., *Science* **277**, 567 (1997); T. F. Franke et al., *Science* **275**, 665 (1997); M. Frech et al., *J. Biol. Chem.* **272**, 8474 (1997); A. Klippel et al., *Mol. Cell Biol.* **17**, 338 (1997); P. J. Coffey, J. Jin, J. R. Woodgett, *Biochem. J.* **335**, 1 (1998); S. J. Isakoff et al., *EMBO J.* **17**, 5374 (1998); J. M. Kavran et al., *J. Biol. Chem.* **273**, 30497 (1998); S. J. Watton and J. Downward, *Curr. Biol.* **9**, 433 (1999).
 22. N. B. Ruderman et al., *Proc. Natl. Acad. Sci. U.S.A.* **87**, 1411 (1990).
 23. M. P. Wymann and L. Pirola, *Biochim. Biophys. Acta* **1436**, 127 (1998).
 24. S. J. Isakoff et al., *EMBO J.* **17**, 5374 (1998).
 25. E. Baraldi et al., *Structure* **7**, 449 (1999).
 26. L. R. Stephens et al., *Cell* **89**, 105 (1997).
 27. A. Ptasnik et al., *J. Biol. Chem.* **271**, 25204 (1996).
 28. T. Sasaki et al., *Science* **287**, 1040 (2000); Z. Li et al., *Science* **287**, 1046 (2000); E. Hirsch et al., *Science* **287**, 1049 (2000).
 29. Yeast cells expressing an exchange factor for Cdc42 that is unable to bind to the G-protein $\beta\gamma$ subunit are unable to orient toward a pheromone gradient [A. Nern and R. A. Arkowitz, *Nature* **391**, 195 (1998)].
 30. Bac1.2F5 macrophages microinjected with a dominant-negative Cdc42 mutant are able to migrate but do not polarize in the direction of the chemotactic gradient [W. E. Allen et al., *J. Cell Biol.* **141**, 1147 (1998)].
 31. Expression of either dominant-positive or dominant-negative Cdc42 mutants render cells of a T cell hybridoma, 2B84, unable to polarize their actin cytoskeleton toward the antigen-presenting cell [L. Stowers, D. Yelon, L. J. Berg, J. Chant, *Proc. Natl. Acad. Sci. U.S.A.* **92**, 5027 (1995)].
 32. We thank C. Bargmann, D. Stokoe, and A. Weiss for critical reading of the manuscript and M. Rosa for support. Supported in part by NIH grants GM-27800 and CA-54427 (H.R.B.), and GM-25101 (J.W.S.). G.S. is a medical Research Council of Canada Postdoctoral Fellow, and O.D.W. is a Howard Hughes Medical Institute Predoctoral Fellow.

4 August 1999; accepted 20 December 1999

Function of PI3K γ in Thymocyte Development, T Cell Activation, and Neutrophil Migration

Takehiko Sasaki,^{1,2} Junko Irie-Sasaki,^{1,2} Russell G. Jones,² Antonio J. Oliveira-dos-Santos,¹ William L. Stanford,³ Brad Bolon,⁴ Andrew Wakeham,¹ Annick Itie,¹ Dennis Bouchard,¹ Ivona Kozieradzki,¹ Nicholas Joza,¹ Tak W. Mak,^{1,2} Pamela S. Ohashi,² Akira Suzuki,^{1,2} Josef M. Penninger^{1,2*}

Phosphoinositide 3-kinases (PI3Ks) regulate fundamental cellular responses such as proliferation, apoptosis, cell motility, and adhesion. Viable gene-targeted mice lacking the p110 catalytic subunit of PI3K γ were generated. We show that PI3K γ controls thymocyte survival and activation of mature T cells but has no role in the development or function of B cells. PI3K γ -deficient neutrophils exhibited severe defects in migration and respiratory burst in response to heterotrimeric GTP-binding protein (G protein)-coupled receptor (GPCR) agonists and chemotactic agents. PI3K γ links GPCR stimulation to the formation of phosphatidylinositol 3,4,5-triphosphate and the activation of protein kinase B, ribosomal protein S6 kinase, and extracellular signal-regulated kinases 1 and 2. Thus, PI3K γ regulates thymocyte development, T cell activation, neutrophil migration, and the oxidative burst.

PI3Ks constitute a family of evolutionarily conserved lipid kinases that regulate a vast array of fundamental cellular responses, including proliferation, transformation, protection from apoptosis, superoxide production,

cell migration, and adhesion (1). These responses result from the activation of membrane-trafficking proteins and enzymes such as the phosphoinositide-dependent kinases (PDKs), protein kinase B (PKB), and S6

REPORTS

Table 1. Blood cell numbers in *PI3Kγ*^{-/-} mice. Seven- to 12-week-old *PI3Kγ*^{+/-} (*n* = 5) and *PI3Kγ*^{-/-} (*n* = 5) littermate mice were used. Bold numbers indicate statistically significant differences between *PI3Kγ*^{+/-} and *PI3Kγ*^{-/-} mice (Mann-Whitney *U* test; *P* < 0.05). Values are given as the mean ± SEM. WBC, white blood cells.

Parameter	<i>PI3Kγ</i> ^{+/-}	<i>PI3Kγ</i> ^{-/-}
Total WBC (× 10 ³ /μl)	3.10 ± 0.44	5.98 ± 1.30
Lymphocytes (× 10 ³ /μl)	2.42 ± 0.38	3.81 ± 1.10
Lymphocytes (% in WBC)	77.8 ± 3.57	54.1 ± 7.92
Neutrophils (× 10 ³ /μl)	0.45 ± 0.10	1.72 ± 0.60
Neutrophils (% in WBC)	14.3 ± 2.20	27.8 ± 6.47
Monocytes (× 10 ³ /μl)	0.05 ± 0.01	0.19 ± 0.06
Monocytes (% in WBC)	1.82 ± 0.26	2.96 ± 0.52
Eosinophils (× 10 ³ /μl)	0.09 ± 0.02	0.60 ± 0.16
Eosinophils (% in WBC)	2.94 ± 0.44	10.4 ± 2.09
Basophils (× 10 ³ /μl)	0.02 ± 0.01	0.02 ± 0.01
Basophils (% in WBC)	0.54 ± 0.07	0.46 ± 0.19
Erythrocytes (× 10 ⁹ /μl)	9.49 ± 0.13	9.06 ± 0.38
Platelets (× 10 ⁷ /μl)	120 ± 5.25	95.9 ± 5.55

kinases (S6Ks) by the key second-messenger phosphatidylinositol 3,4,5-triphosphate [PtdIns (3,4,5)P₃] (2). PtdIns (3,4,5)P₃ is generated from phosphatidylinositol 4,5-bisphosphates through phosphorylation at the 3' position by PI3Ks that are linked to tyrosine kinase-based receptors or G proteins. PI3Kγ is activated in response to GPCRs and can be directly activated by G protein βγ subunits (Gβγ) in vitro (1). The catalytic subunit of PI3Kγ (p110γ) associates with a p101 regulatory subunit but not with the p85 family proteins that regulate other PI3K proteins (3).

To define the physiological roles of PI3Kγ, we disrupted the p110γ catalytic PI3Kγ subunit and generated PI3Kγ null mice (4). Homozygous *PI3Kγ*^{-/-} mice were born at the expected Mendelian ratio, appear healthy, and are fertile. Hematopoietic lineages were examined in peripheral blood and bone marrow of *PI3Kγ*^{+/-} and *PI3Kγ*^{-/-}

Table 2. Cell populations in PI3Kγ-deficient mice. Seven- to 12-week-old *PI3Kγ*^{+/-} and *PI3Kγ*^{-/-} littermate mice were used. Total cells from thymi (*n* = 7), spleens (*n* = 7), lymph nodes (*n* = 3), and bone marrows (*n* = 3) were stained with antibodies against the indicated proteins. Populations were determined by FACScan. Bold numbers indicate statistically significant differences between *PI3Kγ*^{+/-} and *PI3Kγ*^{-/-} mice (Mann-Whitney *U* test; *P* < 0.05). Values are given as the mean ± SEM.

Subsets	<i>PI3Kγ</i> ^{+/-} (% of total)	<i>PI3Kγ</i> ^{-/-} (% of total)
Thymus		
CD4 ⁺ CD8 ⁺	82.3 ± 1.10	77.8 ± 3.25
CD4 ⁺ CD8 ⁻	10.2 ± 0.84	9.77 ± 1.18
CD4 ⁻ CD8 ⁺	1.90 ± 0.08	2.94 ± 0.31
CD4 ⁻ CD8 ⁻	5.55 ± 0.25	9.48 ± 1.78
Spleen		
CD4 ⁺ CD8 ⁻	23.9 ± 2.45	12.9 ± 2.35
CD4 ⁻ CD8 ⁺	8.55 ± 0.96	6.45 ± 1.03
B220 ⁺ sIgM ⁺	34.6 ± 3.12	35.3 ± 1.24
Mac1 ⁺ Gr1 ⁺	1.68 ± 0.11	3.65 ± 0.79
Lymph node		
CD4 ⁺ CD8 ⁻	59.9 ± 2.87	52.3 ± 3.43
CD4 ⁻ CD8 ⁺	15.4 ± 1.53	13.8 ± 0.91
Bone marrow		
B220 ⁺ CD43 ⁺	9.70 ± 1.03	10.7 ± 0.35
B220 ⁺ CD43 ⁻	20.8 ± 5.15	20.4 ± 5.47
Mac1 ⁺ Gr1 ⁺	45.6 ± 7.51	45.3 ± 7.43

littermates. No significant differences in basophil, erythrocyte, or platelet numbers were observed, and all white blood cells exhibited normal morphology on smears stained with Wright-Giemsa or myeloperoxidase. However, PI3Kγ deficiency led to increases in neutrophil, monocyte, and eosinophil populations (Table 1). Total and relative numbers of Gr1⁺Mac1⁺ myeloid cells were also significantly increased in the spleen, but not in bone marrow, of *PI3Kγ*^{-/-} mice (Tables 1 and 2). Thymocyte numbers were significantly reduced in *PI3Kγ*^{-/-} mice (Table 3). The reduction in total thymocyte numbers was also apparent when *PI3Kγ*^{-/-} → *rag1*^{-/-} chimeric mice created by blastocyst complementation were compared to *PI3Kγ*^{+/-} → *rag1*^{-/-} chimeric mice, showing that the developmental defect was intrinsic to thymocytes. Thus, *PI3Kγ*^{-/-} mice exhibit two gross phenotypes: reduced numbers of thymocytes and increased numbers of myeloid

Table 3. Numbers of lymphoid cells in *PI3Kγ*^{-/-} mice. Thymi (*n* = 12), spleens (*n* = 5), and all lymph nodes (*n* = 5) from 4- to 7-week-old *PI3Kγ*^{+/-} and *PI3Kγ*^{-/-} littermate mice or 6-week-old *PI3Kγ*^{+/-} chimeric and *PI3Kγ*^{-/-} chimeric mice (*n* = 4 for all organs) were analyzed. Bold numbers indicate statistically significant differences between *PI3Kγ*^{+/-} and *PI3Kγ*^{-/-} mice or between *PI3Kγ*^{+/-} → *rag1*^{-/-} and *PI3Kγ*^{-/-} → *rag1*^{-/-} chimeric mice (Mann-Whitney *U* test; *P* < 0.05). Values are given as the mean ± SEM.

Lymphatic organ	<i>PI3Kγ</i> ^{+/-}	<i>PI3Kγ</i> ^{-/-}	<i>PI3Kγ</i> ^{+/-} → <i>rag1</i> ^{-/-}	<i>PI3Kγ</i> ^{-/-} → <i>rag1</i> ^{-/-}
Thymus (× 10 ⁶)	2.04 ± 0.27	1.18 ± 0.10	1.53 ± 0.40	0.52 ± 0.20
Spleen (× 10 ⁷)	3.94 ± 0.68	3.70 ± 0.74	2.42 ± 0.71	2.25 ± 0.39
Lymph nodes (× 10 ⁷)	2.68 ± 0.50	2.70 ± 0.52	3.02 ± 0.87	3.15 ± 0.95

cells in the spleen and blood.

In vitro studies indicate that, like PI3Kγ, type-IA PI3Ks can also be activated in response to GPCR stimulation (5). We examined whether PI3Kγ is essential for generating PtdIns (3,4,5)P₃ after GPCR stimulation (6). Receptors of exogenous and endogenous chemoattractants, including the peptide *N*-formyl-Met-Leu-Phe (*f*MPLP) and the complement component C5a are coupled to G protein (G_i). No PtdIns (3,4,5)P₃ accumulation could be detected in PI3Kγ-deficient neutrophils treated with the GPCR agonists *f*MPLP or C5a (Fig. 1A). PI3Ks and PtdIns (3,4,5)P₃ have been implicated in Ca²⁺ mobilization, phosphotyrosine signaling, and the activation of kinases such as PKB, S6Ks, and extracellular signal-regulated kinases 1 and 2 (ERK1 and ERK2, respectively) (1, 2, 7). Stimulation of *PI3Kγ*^{+/-} neutrophils with *f*MPLP or C5a increased kinase activity of PKB (Fig. 1B) and ERK1 and ERK2 (Fig. 1C). In contrast, activation of PKB (Fig. 1B) and phosphorylation of PKB at Ser⁴⁷³ (Fig. 1D) and Thr³⁰⁸ induced by *f*MPLP or C5a were completely abrogated in *PI3Kγ*^{-/-} neutrophils. Phosphorylation of S6K is regulated by PDKs and PKB, both of which are activated by PtdIns (3,4,5)P₃. No S6K phosphorylation was observed in *PI3Kγ*^{-/-} cells (Fig. 1E). Activation (Fig. 1C) and phosphorylation (Fig. 1D) of ERK1 and ERK2 in *PI3Kγ*^{-/-} neutrophils treated with *f*MPLP or C5a were decreased to amounts similar to those observed in wortmannin-treated control cells. Ca²⁺ mobilization (Fig. 1F), activation of p38 kinase, and overall tyrosine phosphorylation induced by *f*MPLP or C5a treatment occurred to the same extent and with the same kinetics in *PI3Kγ*^{+/-} and *PI3Kγ*^{-/-} neutrophils. Activation of PKB in response to the tyrosine kinase-coupled receptor agonist granulocyte-macrophage colony-stimulating factor was comparable in *PI3Kγ*^{+/-} and *PI3Kγ*^{-/-} neutrophils, indicating that the lack of PKB activation in *PI3Kγ*^{-/-} cells in response to GPCR agonists is not due to an intrinsic defect of PKB activation.

To extend the role of PI3Kγ in GPCR signaling to a different cell type, we established bone marrow mast cell (BMMC) lines. BMMCs respond to engagement of the G protein-coupled thrombin receptor, the ty-

¹Amgen Institute, 620 University Avenue, Toronto M5G 2C1, Ontario, Canada. ²Ontario Cancer Institute and the Departments of Medical Biophysics and Immunology; ³Samuel Lunenfeld Research Institute, Mount Sinai Hospital, and Department of Medical Genetics, University of Toronto, Toronto M5G 2C1, Ontario, Canada. ⁴Department of Pathology, Amgen, One Amgen Center Drive, Thousand Oaks, CA 91320-1789, USA.

*To whom correspondence should be addressed. E-mail: jpenning@amgen.com

REPORTS

rosine kinase-based receptors for c-Kit, interleukin-3 (IL-3), and immunoglobulin E (IgE) (8). Stimulation of *PI3K γ ^{+/-}* BMMCs with thrombin, stem cell factor (SCF or c-Kit ligand), IL-3, and IgE led to phosphorylation of PKB and ERK1 and ERK2 (Fig. 1G). Phosphorylation of ERK1 and ERK2 and PKB induced by the GPCR agonist thrombin

was abolished in *PI3K γ ^{-/-}* BMMCs (Fig. 1G). Thrombin did not activate type-IA PI3Ks in BMMCs assessed by PI3K activity present in antiphosphotyrosine immunoprecipitates (Fig. 1H). SCF-stimulated activation of type-IA PI3Ks occurred equally well in *PI3K γ ^{-/-}* and control BMMC. These data show that PI3K γ is the essential lipid kinase

linking GPCRs to PtdIns (3,4,5)P₃ accumulation and activation of PKB and S6K.

To determine the role of PI3K γ in the inflammatory response, we examined neutrophil migration in experimental models of peritonitis in vivo. Accumulation of neutrophils in the peritoneal cavities was significantly reduced in both casein- and *Listeria*

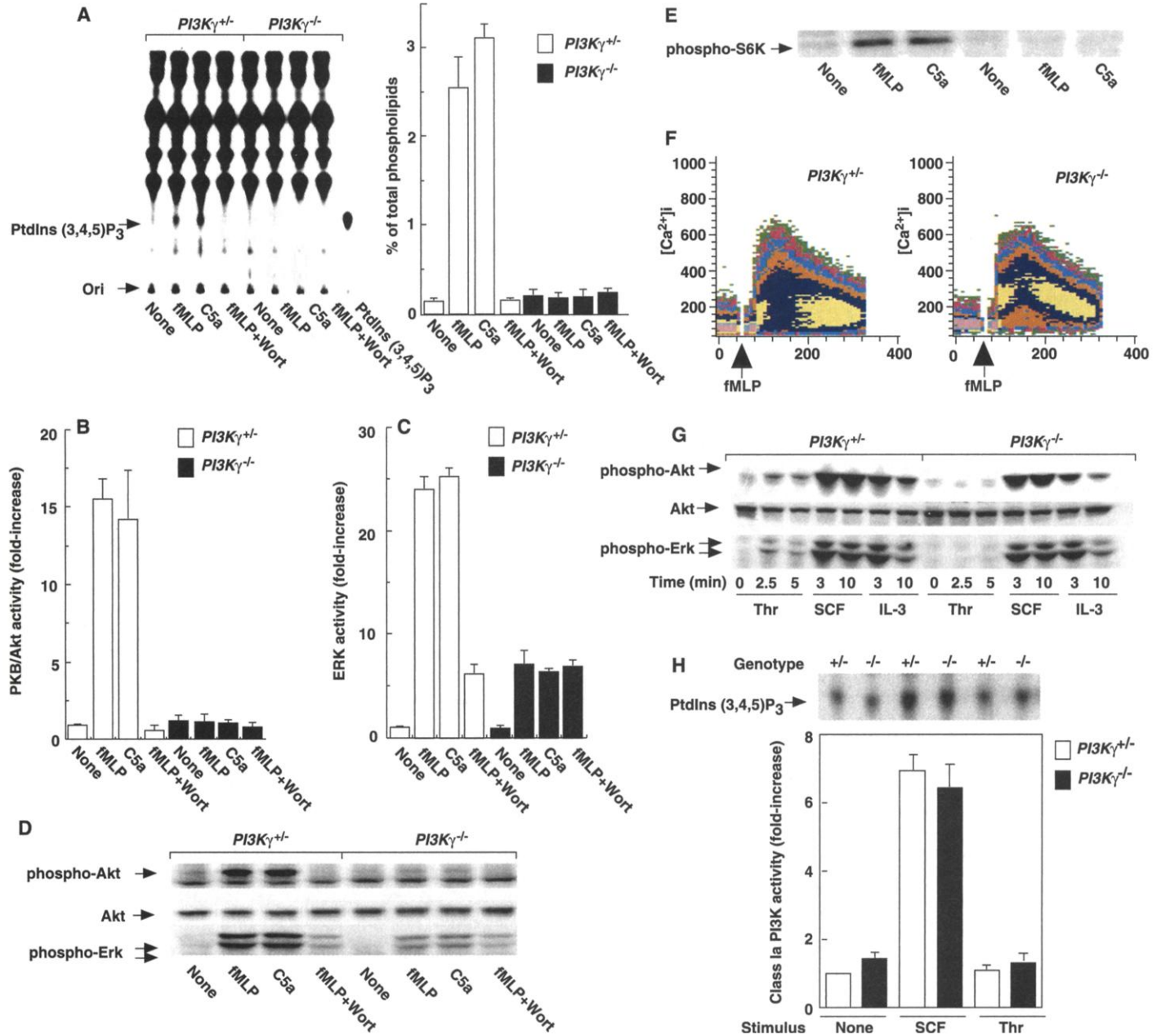


Fig. 1. PI3K γ regulates PtdIns (3,4,5)P₃ production and activation of PKB and ERKs. (A) Failure of *PI3K γ ^{-/-}* neutrophils to produce PtdIns (3,4,5)P₃. Cells labeled with ³²P were incubated with or without wortmannin (wort, 100 nM) for 10 min before stimulation with fMLP (8 μ M) or C5a (100 ng/ml). Left panel, thin-layer chromatography. Ori, origin. Right panel, PtdIns (3,4,5)P₃ quantitation. (B through E) Activation of PKB [(B) and (D)], ERK1 and ERK2 [(C) and (D)], and S6K (E). Neutrophils were incubated with or without wortmannin (wort, 100 nM) before stimulation with fMLP (8 μ M) or C5a (100 ng/ml). PKB and ERK1 and ERK2 activation were determined in triplicate by in vitro kinase assays and with phospho-specific antibodies against PKB (Ser⁴⁷³), ERK1 and ERK2 (Thr²⁰²/Tyr²⁰⁴), and S6K (Thr⁴²¹/Ser⁴²⁴). (F) Ca²⁺ mobilization. Indo-1-loaded neutrophils were stimulated with 8 μ M

fMLP, and Ca²⁺ flux was monitored in real time by FACS. Arrows indicate the time of fMLP addition. (G) GPCR agonist-specific activation of PKB and ERK1 and ERK2. Serum-starved BMMCs were treated with thrombin (Thr, 5 units/ml), SCF (100 ng/ml), or IL-3 (5 ng/ml). Phosphorylation of PKB and ERK1 and ERK2 was monitored by phospho-specific antibodies. (H) In vitro PI3K activity. BMMCs were left untreated (none), or activated with SCF (100 ng/ml) or thrombin (Thr, 5 units/ml) for 1 min. Total phosphorylated proteins were immunoprecipitated with an antibody to phosphotyrosine, and the associated PI3K activity was determined. Baseline p85 α /PI3K activity was similar in *PI3K γ ^{+/-}* and *PI3K γ ^{-/-}* BMMCs. Upper panel, thin-layer chromatography; lower panel, quantitation of PtdIns (3,4,5)P₃. Error bars in (A), (B), (C), and (H) indicate \pm SD.

monocytogenes-treated $PI3K\gamma^{-/-}$ mice in comparison to control animals (Fig. 2A). We further tested purified neutrophils for in vitro chemotaxis in response to GPCR agonists. *f*MPLP- and C5a-induced chemotaxis of neutrophils from $PI3K\gamma^{-/-}$ mice were decreased by 70% in comparison to neutrophils from heterozygous littermates (Fig. 2B). $PI3K\gamma^{-/-}$ neutrophils adhered to fibronectin-coated surfaces as tightly as $PI3K\gamma^{+/-}$ cells (9), suggesting that the decreased chemotaxis in $PI3K\gamma^{-/-}$ neutrophils is due to impaired motility and not altered adhesion. These in vivo and in vitro results identify $PI3K\gamma$ as a critical link between GPCR stimulation and the chemotactic response.

In addition to chemotaxis, it has been reported that PI3Ks link stimulation of GPCRs to respiratory burst (superoxide anion O_2^- production) (10). GPCR-induced respiratory burst was decreased in freshly isolated bone marrow neutrophils from $PI3K\gamma^{-/-}$ mice (Fig. 2C). The direct protein kinase C-activator phorbol 12-myristate 13-acetate (PMA) induced superoxide anion formation

in both $PI3K\gamma^{-/-}$ and $PI3K\gamma^{+/-}$ neutrophils. Thus, GPCR-triggered respiratory burst depends on $PI3K\gamma$. However, the requirement of $PI3K\gamma$ for oxidative burst is not absolute because primed neutrophils isolated from the peritoneal cavity still produce O_2^- in response to C5a and *f*MPLP. $PI3K\gamma^{-/-}$ neutrophils were able to ingest IgG-coated particles as readily as $PI3K\gamma^{+/-}$ cells (Fig. 2D), suggesting that $PI3K\gamma$ does not act downstream of these tyrosine kinase-based receptors. The kinetics and extents of apoptosis were comparable among freshly isolated total myeloid cells and neutrophils from the spleens of $PI3K\gamma^{+/-}$ and $PI3K\gamma^{-/-}$ mice. Thus, in neutrophils, $PI3K\gamma$ links GPCRs to cell migration and superoxide formation.

In addition to neutrophil defects, $PI3K\gamma^{-/-}$ mice exhibit a reduction in thymic cellularity (Table 3). Thymocytes undergo defined stages of development, from $CD4^-CD8^-$ double-negative (DN) precursors to $CD4^+CD8^+$ double-positive (DP) immature thymocytes, and finally, they mature to single-positive (SP)

$CD4^+$ or $CD8^+$ T cells (11). The proportions of mature $CD4^+$ and $CD8^+$ SP thymocytes were equal in $PI3K\gamma^{-/-}$, $PI3K\gamma^{+/-}$, and $PI3K\gamma^{-/-} \rightarrow rag1^{-/-}$ mice. There was a slight decrease in the proportion of DP cells and an increase in DN cells (Table 2). No differences were found in the amount of $\alpha\beta$ T cell receptor (TCR $\alpha\beta$), CD3, CD4, CD8, CD28, CD45, TCRV β subclasses, and CD95 expressed on the surface of SP and DP thymocytes. The maturation of DN precursor populations (defined by surface expression of CD44 and CD25), maturation of DP thymocytes to SP thymocytes (defined by expression of CD69, CD44, heat stable antigen, CD5, and H2-K^b); and proliferation of DN precursors and mature thymocytes were similar among $PI3K\gamma^{+/-}$, $PI3K\gamma^{+/-}$, and $PI3K\gamma^{-/-}$ mice (12). These data suggest that early thymocyte development and progression from DP to mature thymocytes do not require $PI3K\gamma$.

It is estimated that 90 to 95% of DP thymocytes are lost to apoptotic "death by neglect" due to the expression of nonfunctional antigen receptors (11). To examine the impact of $PI3K\gamma$ deficiency on thymocyte survival, we evaluated DP thymocyte apoptosis to treatment with antibodies to CD3 ϵ and Fas, γ irradiation, or dexamethasone (13). No differences in the kinetics or extents of apoptosis were observed between mutant and control mice (Fig. 3A). Human patients with mutations in adenosine deaminase exhibit severe combined immunodeficiency disease and a defect in thymocyte maturation (14). Adenosine is naturally present in thymi in vivo, and the adenosine A2A receptor is expressed on thymocytes. The adenosine A2A receptor is a GPCR that can activate adenylate cyclase and $PI3K\gamma$ (15). Stimulation of $PI3K\gamma^{+/-}$ thymocytes with adenosine A2A receptor agonists *N*6-[4-[[[4-[[[2-aminoethyl]amino]carbonyl]methyl]-anilino]carbonyl]methyl]phenyl]adenosine (ADAC) or 2-*p*-(2-carboxyethyl)phenethylamino-5'-*N*-ethylcarboxamidoadenosine hydrochloride (CGS) caused a small amount of cell death (Fig. 3A). However, $PI3K\gamma^{-/-}$ thymocytes exhibited much more apoptosis after stimulation with either adenosine receptor agonist (Fig. 3A). Treatment of thymocytes with ADAC or CGS with antibody to CD3 ϵ (anti-CD3 ϵ) slightly increased the death of $PI3K\gamma^{+/-}$ cells but substantially increased cell death of $PI3K\gamma^{-/-}$ thymocytes (Fig. 3B). We further investigated the influence of $PI3K\gamma$ on thymocyte apoptosis in vivo by injecting control and mutant mice with monoclonal antibodies (mAbs) to CD3 ϵ , which results in apoptosis of DP thymocytes (16). In $PI3K\gamma^{-/-}$ mice, not only was the total number of thymocytes decreased, but also the specific depletion of the DP population was enhanced in comparison to that in $PI3K\gamma^{+/-}$ mice (Fig. 3, C and D). These results indicate that $PI3K\gamma$ has a role in the maintenance of homeostasis of the

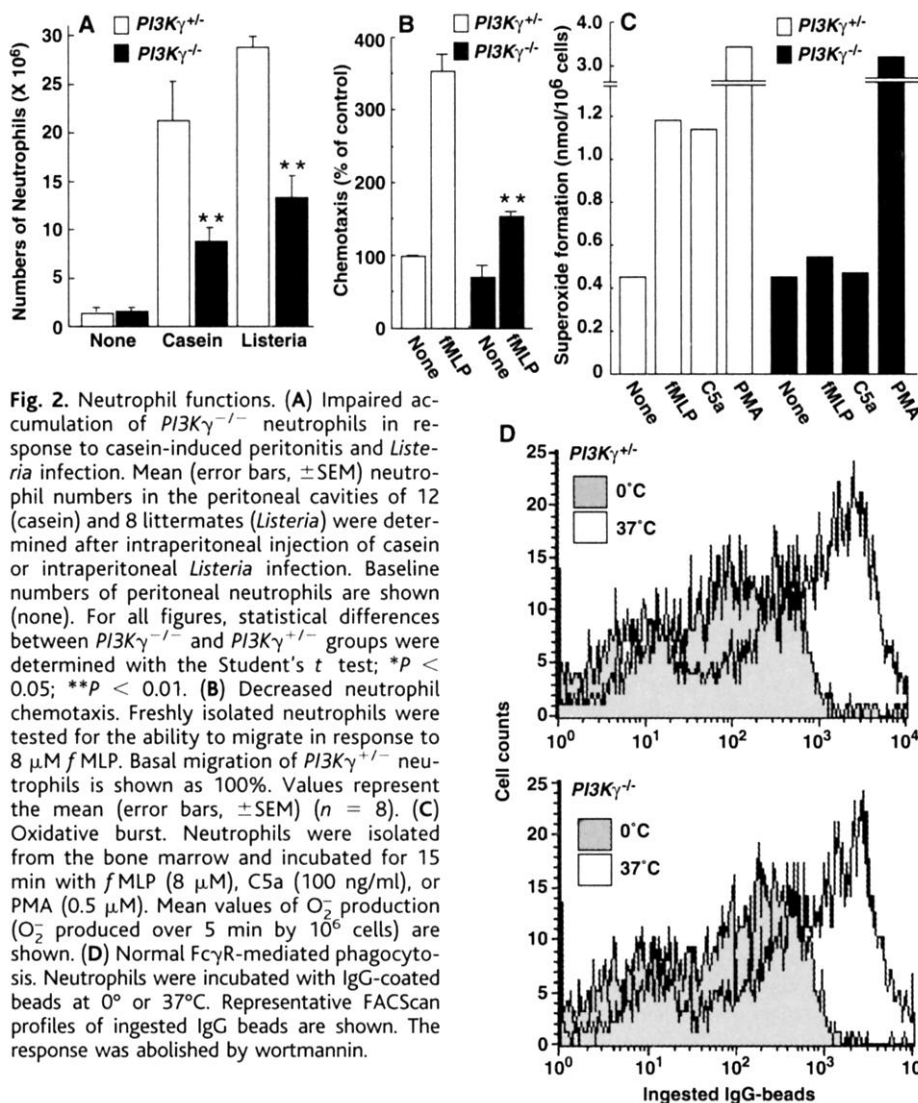


Fig. 2. Neutrophil functions. (A) Impaired accumulation of $PI3K\gamma^{-/-}$ neutrophils in response to casein-induced peritonitis and *Listeria* infection. Mean (error bars, \pm SEM) neutrophil numbers in the peritoneal cavities of 12 (casein) and 8 littermates (*Listeria*) were determined after intraperitoneal injection of casein or intraperitoneal *Listeria* infection. Baseline numbers of peritoneal neutrophils are shown (none). For all figures, statistical differences between $PI3K\gamma^{-/-}$ and $PI3K\gamma^{+/-}$ groups were determined with the Student's *t* test; **P* < 0.05; ***P* < 0.01. (B) Decreased neutrophil chemotaxis. Freshly isolated neutrophils were tested for the ability to migrate in response to 8 μ M *f*MPLP. Basal migration of $PI3K\gamma^{+/-}$ neutrophils is shown as 100%. Values represent the mean (error bars, \pm SEM) (*n* = 8). (C) Oxidative burst. Neutrophils were isolated from the bone marrow and incubated for 15 min with *f*MPLP (8 μ M), C5a (100 ng/ml), or PMA (0.5 μ M). Mean values of O_2^- production (O_2^- produced over 5 min by 10⁶ cells) are shown. (D) Normal Fc γ R-mediated phagocytosis. Neutrophils were incubated with IgG-coated beads at 0 $^\circ$ or 37 $^\circ$ C. Representative FACS profiles of ingested IgG beads are shown. The response was abolished by wortmannin.

REPORTS

thymus by regulating TCR- and GPCR-induced thymocyte apoptosis.

Gene targeting of the PI3K subunit p85 α leads to a block in early B cell development and defective proliferation of mature B cells in response to IL-4, CD40, and B cell receptor (BCR) (anti-IgM) stimulation (17). Development, proliferation, and IL-2 production of T cells appeared normal in *p85 α ^{-/-}* mice, although inhibition of PI3K with wortmannin partially inhibits T cell proliferation and cytokine production after TCR and CD28 stimulation. *PI3K γ ^{-/-}* and *PI3K γ ^{-/-} → rag1^{-/-}* chimeric mice displayed normal numbers and differentiation of B220⁺CD25⁺, B220⁺CD25⁻, B220⁺CD43⁺, B220⁺CD43⁻, B220⁺sIgM⁺, and CD19⁺sIgM⁺sIgD⁺ B cells in the bone marrow (sIg, surface Ig); conventional CD19⁺sIgM⁺sIgD⁺CD23⁺ B cells in peripheral lymphoid organs; and B1 (CD5⁺IgM⁺) B cells in the peritoneal cavity (Tables 2 and 3). Proliferation of *PI3K γ ^{-/-}* B cells in response to a mAb to IgM, the F(ab')₂ fragment of the antibody to IgM, anti-CD40 (Fig. 4A), IL-4, or lipopolysaccharide was similar to that of *PI3K γ ^{+/-}* B cells (18). These data show that PI3K γ has no apparent role in B cell development or in BCR- or CD40-mediated B cell proliferation.

In contrast to B cells, thymic development was altered in *PI3K γ ^{-/-}* mice. Lymph nodes of *PI3K γ ^{-/-}* mice contained normal numbers and ratios of CD4⁺ and CD8⁺ T cells. However, CD4⁺ T cells, but not CD8⁺ T cells, were reduced in *PI3K γ ^{-/-}* spleens (Table 2). The amounts of TCR $\alpha\beta$, CD3, CD4, CD8, CD28, CD45, CD44, LFA-1, CD25, and CD69 on the surface of both splenic and lymph node CD4⁺ and CD8⁺ T cells were comparable in *PI3K γ ^{+/-}* and *PI3K γ ^{-/-}* mice. Whereas *PI3K γ ^{+/-}* and *PI3K γ ^{-/-}* T cells proliferated equally well in response to stimulation by PMA/Ca²⁺ ionophore, *PI3K γ ^{-/-}* T cells showed impaired proliferation in response to anti-CD3 ϵ or concanavalin A (Con A) stimulation (Fig. 4B) (18). The engagement of the costimulatory CD28 receptor increased TCR/CD3-mediated proliferation in both *PI3K γ ^{+/-}* and *PI3K γ ^{-/-}* T cells and rescued the proliferation defect of *PI3K γ ^{-/-}* T cells (Fig. 4B). Nevertheless, *PI3K γ ^{-/-}* T cells produced lower amounts of IL-2 (Fig. 4C) and interferon- γ (IFN- γ) (Fig. 4D) in response to treatment with anti-CD3 ϵ and anti-CD28 or Con A. The efficacy of splenic antigen-presenting cells to induce proliferation and IL-2 production was comparable between *PI3K γ ^{+/-}* and *PI3K γ ^{-/-}* mice with mixed lymphocyte reactions (18). The functional defect in cytokine production can also be observed in *PI3K γ ^{-/-}* T cells treated with PMA/Ca²⁺ ionophore, a stimulus that bypasses the initial TCR signal (Fig. 4, C and D). Moreover, TCR-mediated Ca²⁺ flux, tyrosine phosphorylation, and activation of tyrosine kinases were comparable among

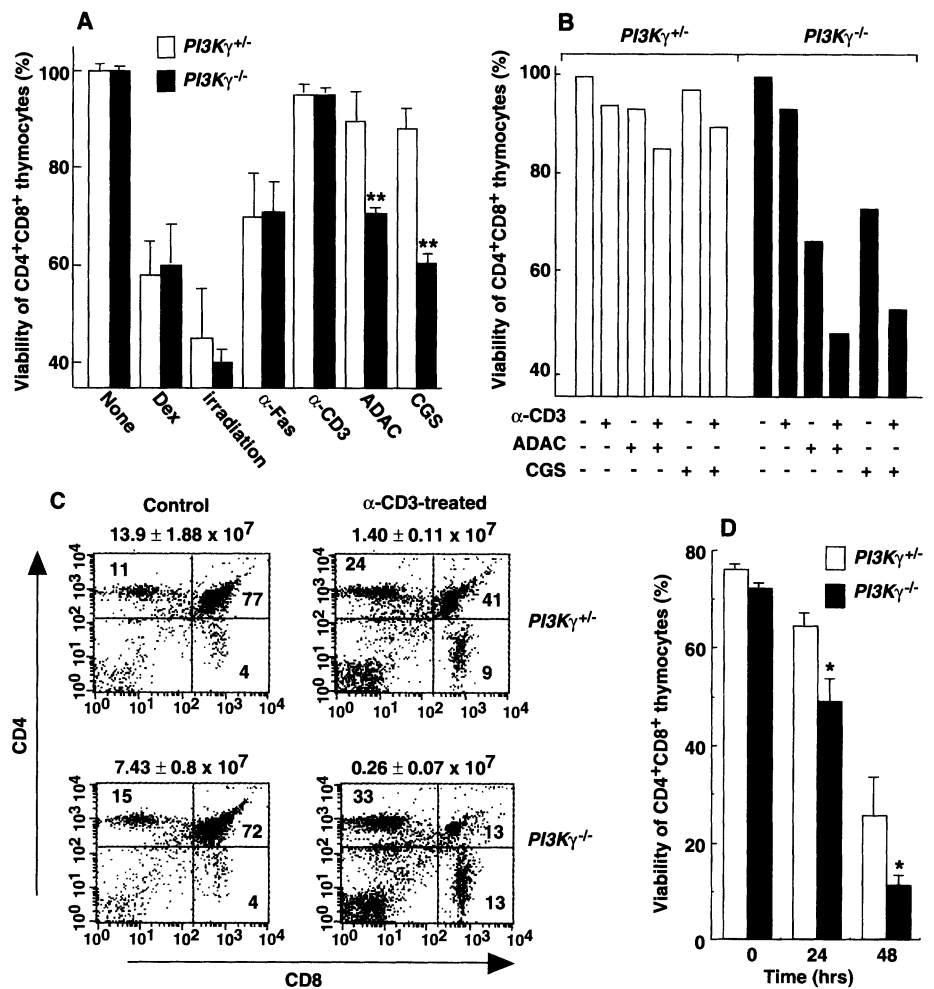


Fig. 3. PI3K γ regulates thymocyte survival (A) Increased susceptibility of *PI3K γ ^{-/-}* thymocytes to adenosine receptor-mediated apoptosis. Freshly isolated thymocytes were stimulated for 20 hours with dexamethasone (0.1 μ M), γ irradiation (5 Gy), anti-CD95 (FAS, 1 μ g/ml), immobilized anti-CD3 ϵ (0.1 μ g/ml), or the adenosine receptor agonists ADAC (10 μ M) or CGS (10 μ M). Mean percentages (error bars, \pm SD) of viable DP thymocytes are indicated (14). Spontaneous apoptosis was comparable among nonstimulated *PI3K γ ^{+/-}* and *PI3K γ ^{-/-}* thymocytes. (B) Adenosine receptor agonists increase anti-CD3-mediated cell death. Thymocytes were cultured for 20 hours in medium alone (-) or in the presence of (+) immobilized anti-CD3 ϵ (0.1 μ g/ml), ADAC (10 μ M), CGS (10 μ M), or anti-CD3 ϵ plus adenosine analogs. Percent viability of DP thymocytes (14) was normalized to the percentage of viable DP cells in untreated cultures (100%). (C) Increased anti-CD3-mediated cell death in vivo. Total thymocytes were isolated from mice 48 hours after intraperitoneal injection with phosphate-buffered saline (PBS) (control) or mAb to CD3 ϵ (50 μ g/200 μ l PBS). Cells were stained with anti-CD4-PE, anti-CD8-FITC, and 7-AAD and analyzed by FACS. Percentages of different thymocyte subpopulations in gated live cells are shown within quadrants. Numbers above panels indicate total numbers of viable DP cells (mean \pm SD) (n = 6 mice per group). (D) Time course of anti-CD3-mediated cell death in vivo. Total thymocytes were isolated from mice at 0, 24, or 48 hours after intraperitoneal injection with anti-CD3 ϵ (50 μ g/200 μ l PBS). Mean percentages (error bars, \pm SD) of DP thymocytes that remained viable from four (24 hours) and six (48 hours) independent experiments are shown.

PI3K γ ^{+/-} and *PI3K γ ^{-/-}* T cells. Thus, it appears that PI3K γ does not act downstream of the TCR but regulates a second signal through GPCRs.

To examine the role of PI3K γ in T cell responses in vivo, we injected *PI3K γ ^{+/-}* and *PI3K γ ^{-/-}* mice in the footpad with lymphocytic choriomeningitis virus (LCMV) (19). The early phase (days 6 to 8 after infection) of this footpad-swelling reaction is mediated by CD8⁺ cytotoxic T lymphocytes (CTLs), whereas the later phase depends on CD4⁺ T cells (20).

Whereas *PI3K γ ^{+/-}* mice developed an effective LCMV-induced footpad-swelling reaction starting from day 6 after infection, footpad swelling was reduced in *PI3K γ ^{-/-}* mice (Fig. 4E). T cells recovered from the spleens of both *PI3K γ ^{+/-}* and *PI3K γ ^{-/-}* mice generated a normal primary cytotoxic response to LCMV peptides (Fig. 4F). *PI3K γ ^{+/-}* and *PI3K γ ^{-/-}* mice were further immunized with the T helper cell-dependent hapten nitroiodophenylacetic acid conjugated to ovalbumin (NIP-OVA). Whereas *PI3K γ ^{+/-}* mice exhibited high titers

REPORTS

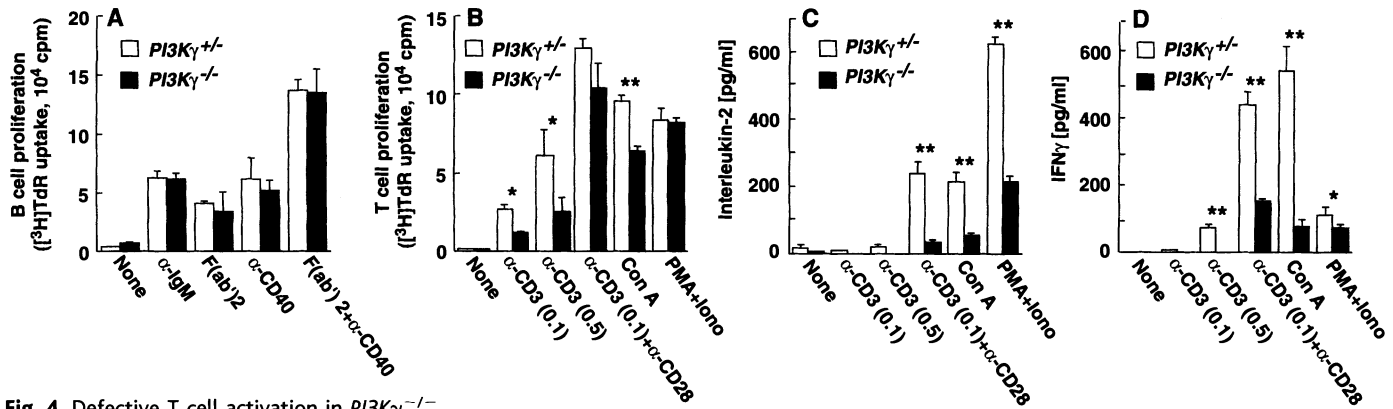
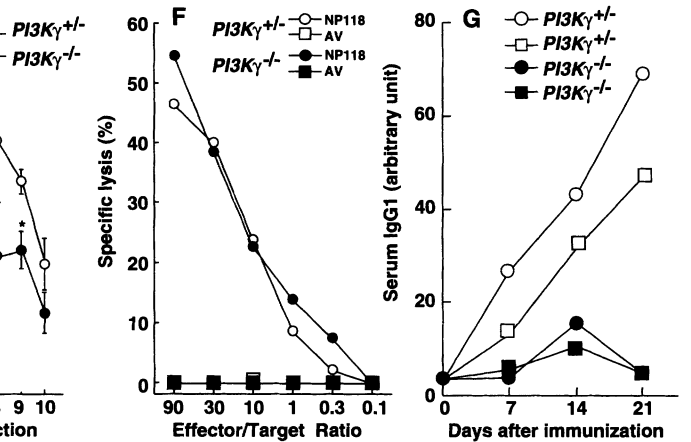


Fig. 4. Defective T cell activation in $PI3K\gamma^{-/-}$ mice. (A) B cell activation. Purified spleen B cells (1×10^5 per well) were incubated for 36 hours in medium alone (none), anti-IgM (20 μ g/ml), anti-IgM F(ab')₂ [F(ab')₂, 15 μ g/ml], anti-CD40 (5 μ g/ml), or anti-IgM F(ab')₂ [F(ab')₂, 15 μ g/ml] plus anti-CD40 (5 μ g/ml). Mean values of [³H]-thymidine uptake (error bars, \pm SD) are shown. Similar results were observed for various seeding numbers and at earlier and later time points of activation. (B) Proliferation and (C) IL-2, and (D) IFN- γ production. T cells were purified from lymph nodes and activated with anti-CD3 ϵ (0.1 or 0.5 μ g/ml), anti-CD3 ϵ (0.1 μ g/ml) plus anti-CD28 (20 ng/ml), Con A (2 μ g/ml), and PMA (10 ng/ml) plus Ca²⁺ ionophore (100 ng/ml) (PMA+Iono). Culture supernatants were analyzed after 24 hours for cytokine production by ELISA. Proliferation was determined at 48 hours. Values are the means (error bars, \pm SEM) of triplicate cultures. Phenotypes and activation status of input T and B cells populations were similar between $PI3K\gamma^{+/+}$ and $PI3K\gamma^{-/-}$ mice. (E) Footpad-swelling reaction. Mice were inoculated with 2000 PFU of LCMV, and swelling was assessed daily. Mean values (error bars, \pm SEM) from five $PI3K\gamma^{+/+}$ and five $PI3K\gamma^{-/-}$ littermates are shown. (F) Cytotoxicity. Mice were inoculated with LCMV as in (E).



Spleen cells were harvested 10 days later, and cytotoxicity was measured using EL-4 target cells pulsed with the LCMV-specific peptide NP118-126 or the nonspecific peptide AV. (G) Responses to the T cell-dependent hapten NIP-OVA. Serum IgG1 titers were determined 7, 14, and 21 days after immunization. Arbitrary units of optical density (at 405 nm) of NIP-specific IgG1 titers are shown for individual mice.

of antibodies to NIP-specific IgG1, antibodies to NIP were reduced in $PI3K\gamma^{-/-}$ mice (Fig. 4G). Thus, $PI3K\gamma$ is required to generate effective CD8⁺ T cell-dependent antiviral responses and functional T helper cell-dependent responses to hapten antigens in vivo.

$PI3Ks$ link surface receptors to phosphatidylinositol-regulated signaling pathways. We report the generation of viable mice lacking the p110 γ catalytic $PI3K$ subunit ($PI3K\gamma^{-/-}$). $PI3K\gamma^{-/-}$ mice display two principal phenotypes: accumulation of neutrophils and reduced thymic cellularity. Neutrophils had defects in migration and oxidative burst in response to agonists that trigger GPCRs. $PI3K\gamma$ mediates PtdIns (3,4,5)P₃ production and activation of PKB and S6K in response to the GPCR agonists C5a, fMLP, and thrombin in neutrophils and mast cells. In addition, $PI3K\gamma$ is critical for GPCR-triggered activation of ERK1 and ERK2. In contrast to mutation of p85 α (the regulatory subunit of $PI3K\alpha$, $PI3K\beta$, and $PI3K\delta$, which leads to developmental and functional defects in B cells, but not in T cells), deletion of $PI3K\gamma$ had no effect on B lymphocytes. Instead, $PI3K\gamma$ regulates proliferation and cytokine production of T lymphocytes.

Moreover, $PI3K\gamma$ expression is required for an effective T cell-dependent footpad-swelling reaction following viral challenge and functional T helper cell-dependent responses to hapten antigens in vivo. In thymocytes, $PI3K\gamma$ provides a developmental survival signal.

References and Notes

- A. Toker and L. C. Cantley, *Nature* **387**, 673 (1997); L. R. Stephens, T. R. Jackson, P. T. Hawkins, *Biochim. Biophys. Acta* **1179**, 27 (1993).
- T. F. Franke, D. R. Kaplan, L. C. Cantley, *Cell* **88**, 435 (1997); D. R. Alessi, M. T. Kozlowski, Q. P. Weng, N. Morrice, J. Avruch, *Curr. Biol.* **8**, 69 (1998); J. Downward, *Science* **279**, 673 (1998).
- B. Stoyanov et al., *Science* **269**, 690 (1995); L. R. Stephens et al., *Cell* **89**, 105 (1997).
- For generation of $PI3K\gamma$ mutant mice, see supplementary material (available at www.sciencemag.org/feature/data/1045107.shl).
- H. Kurosu et al., *J. Biol. Chem.* **272**, 24252 (1997); Z. K. Pan, S. C. Christiansen, A. Ptasznik, B. L. Zuraw, *J. Biol. Chem.* **274**, 9918 (1999).
- Signal transduction was as follows. Neutrophils and BMDCs were isolated, and phosphorylation was detected by phospho-specific antibodies as described (27). PKB and ERK1 and ERK2 activation were determined by in vitro kinase assays with histone H2 and myelin basic protein as substrates. Protein levels of p85 α , p110 α , p110 β , and p110 γ were determined by Western blotting. Cellular PtdIns (3,4,5)P₃ levels and $PI3K$ activity were measured as described (22).
- N. Pullen et al., *Science* **279**, 707 (1998).

- C. D. Helgason et al., *Genes Dev.* **12**, 1610 (1998).
- For in vivo neutrophil migration, mice were injected intraperitoneally with 1 ml of 9% casein or infected with 1×10^7 *L. monocytogenes*. Neutrophils were isolated by peritoneal lavage and purified by Percoll density gradient centrifugation. For oxidative burst studies, neutrophils were freshly purified from bone marrow, and cytochrome C reduction was determined by spectroscopy at 550 to 540 nm (in nmol of O₂²⁻ produced over 5 min by 10⁶ cells). For cell adhesion studies, neutrophils were placed into flat-bottomed 96-well plates coated with fibronectin (10 μ g/ml), and the percentage of adherent cells relative to input was determined by XTT assay (Boehringer Mannheim). Fc γ R-mediated phagocytosis of neutrophils was measured with Fc-OxyBURST reagents (Molecular Probes, Eugene, OR). Chemotaxis assays were carried out with 24-well Transwell chambers (8.0 μ m).
- T. Okada, L. Sakuma, Y. Fukui, O. Hazeki, M. Ui, *J. Biol. Chem.* **269**, 3563 (1994); M. Thelen, M. P. Wymann, H. Langen, *Proc. Natl. Acad. Sci. U.S.A.* **91**, 4960 (1994).
- S. Mariathasan, R. G. Jones, P. S. Ohashi, *Semin. Immunol.* **11**, 263 (1999).
- Immunocytochemistry was performed as follows. Cell suspensions of thymic, lymph nodes, bone marrow, blood, and spleens were stained with fluorescein isothiocyanate (FITC)-, phycoerythrin (PE)-, or biotin-conjugated antibodies to cell surface molecules. For the analysis of thymocyte precursors, cells were stained with PE-conjugated anti-CD4, anti-CD8, anti-CD3 ϵ , anti-B220, anti-CD11b, anti-Gr-1, and anti-TCR $\gamma\delta$; FITC-conjugated anti-CD25; and biotin-conjugated anti-CD44. PE-negative precursor cells were

- analyzed for expression of CD25 and CD44. Biotinylated antibodies were visualized with streptavidin-RED670. Samples were analyzed by FACScan.
13. For the analysis of apoptosis, thymocytes were cultured for various times in 24-well flat-bottomed tissue culture plates at a density of 2×10^6 cells/ml in Iscove's modified Dulbecco's medium (10% fetal calf serum) and treated with apoptotic stimuli. Cells were harvested; stained with the 7-amino-actinomycin D (7-AAD), anti-CD4, and anti-CD8; and subjected to fluorescence-activated cell sorting (FACS) analysis. Apoptosis was confirmed with annexin V, propidium iodide, trypan blue, and 3,3'-dipropylloxycarbocyanine iodide.
 14. D. Cournoyer and C. T. Caskey, *Annu. Rev. Immunol.* **11**, 297 (1993).
 15. S. Huang, S. Apasov, M. Koshiba, M. Sitkovsky, *Blood* **90**, 1600 (1997).
 16. M. Rincon *et al.*, *J. Exp. Med.* **188**, 1817 (1998).
 17. D. A. Fruman *et al.*, *Science* **283**, 393 (1999); H. Suzuki *et al.*, *Science* **283**, 390 (1999).
 18. Lymphocyte proliferation and cytokine production were determined as described (21). For mixed lymphocyte reactions, T cell-depleted, irradiated [20 grays (Gy)] splenic antigen-presenting cells from H-2^{b/b} PI3K $\gamma^{+/-}$ and PI3K $\gamma^{-/-}$ mice were used as stimulators for allogeneic (H-2^{d/d} and H-2^{k/k}) wild-type T cells.
 19. Virus infections and hapten immunization were as follows. Mice were inoculated in one hind footpad with 2000 plaque-forming units (PFU) of LCMV-Armstrong (LCMV-Arm) in 30 μ l of Hank's balanced salt solution. Footpad swelling was assessed daily with a spring-loaded caliper (20). LCMV-specific CTL activity of spleen cells was determined 10 days after infection by a ⁵¹Cr-release assay with EL-4 target cells coated with the LCMV peptide NP118-126 or the nonspecific peptide AV (10^{-6} M). Percent specific ⁵¹Cr release was calculated as [(experimental release

- spontaneous release) \times 100/(total release – spontaneous release)]. For hapten immunization, male mice were intraperitoneally immunized with 100 μ g of the T cell-dependent haptenated protein NIP-OVA. NIP-specific IgG1 titers were determined by enzyme-linked immunosorbent assay (ELISA) on plates coated with NIP-bovine serum albumin.
20. W. P. Fung-Leung, T. M. Kündig, R. M. Zinkernagel, T. W. Mak, *J. Exp. Med.* **174**, 1425 (1991).
 21. Y. Y. Kong *et al.*, *Nature* **397**, 315 (1999).
 22. Q. Liu *et al.*, *Genes Dev.* **13**, 786 (1999); T. Sasaki, K. Hazeki, O. Hazeki, M. Ui, T. Katada, *Biochem. J.* **315**, 1035 (1996).
 23. We thank M. Saunders, K. Bachmaier, Y. Kong, M. Crackover, E. Griffith, Q. Liu, V. Stambolic, L. Zhang, G. Duncan, C. Krawczyk, and D. Lacey for comments. T.S., J.L.-S., and J.M.P. are supported by the Medical Research Council and National Cancer Institute of Canada and by Amgen.

3 September 1999; accepted 16 December 1999

Roles of PLC- β 2 and - β 3 and PI3K γ in Chemoattractant-Mediated Signal Transduction

Zhong Li,^{1,2*} Huiping Jiang,^{1*†} Wei Xie,^{1*} Zuchuan Zhang,¹ Alan V. Smrcka,¹ Dianqing Wu^{1,2‡}

The roles of phosphoinositide 3-kinase (PI3K) and phospholipase C (PLC) in chemoattractant-elicited responses were studied in mice lacking these key enzymes. PI3K γ was required for chemoattractant-induced production of phosphatidylinositol 3,4,5-trisphosphate [PtdIns (3,4,5)P₃] and has an important role in chemoattractant-induced superoxide production and chemotaxis in mouse neutrophils and in production of T cell-independent antigen-specific antibodies composed of the immunoglobulin λ light chain (TI-Ig λ _L). The study of the mice lacking PLC- β 2 and - β 3 revealed that the PLC pathways have an important role in chemoattractant-mediated production of superoxide and regulation of protein kinases, but not chemotaxis. The PLC pathways also appear to inhibit the chemotactic activity induced by certain chemoattractants and to suppress TI-Ig λ _L production.

Chemoattractants have important roles in inflammatory reactions. Their receptors couple to the inhibitory heterotrimeric guanine nucleotide-binding proteins (G_i proteins) and elicit a wide range of responses in leukocytes (1–3). It is thought that two signaling pathways mediated by PLC (4) and PI3K (5, 6) are activated by chemoattractant receptors. To investigate the role of the PI3K-linked pathway in chemoattractant-mediated responses, we generated a mouse line that lacks PI3K γ . A gene-targeting vector was constructed so that a green fluorescence protein (GFP) coding sequence was fused with the coding

frame of PI3K γ (Fig. 1A). Thus, the expression of GFP is under the control of the endogenous PI3K γ promoter in the transgenic mice. The mice heterozygous and homozygous for the disrupted PI3K γ genes were generated as described (7), and the genotypes were verified with Southern cDNA and Western blot analyses (Fig. 1A).

To determine the contribution of PI3K γ to chemoattractant-induced PtdIns (3,4,5)P₃ production in mouse neutrophils, we compared formyl peptide *N*-formyl-Met-Leu-Phe (*f*MLP)-induced PtdIns (3,4,5)P₃ production in neutrophils from either wild-type or PI3K γ -deficient mice (8). The neutrophils were prepared from the peritonea of mice treated with 2% casein (9). Although *f*MLP-elicited production of PtdIns (3,4,5)P₃ was clearly detected in the wild-type neutrophils, no production of PtdIns (3,4,5)P₃ was detected in response to *f*MLP in cells lacking PI3K γ (Fig. 1B). This result indicates that PI3K γ is the predominant PI3K isoform that mediates *f*MLP-induced PtdIns (3,4,5)P₃

production in mouse neutrophils.

The expression of PI3K γ in mice was examined by detecting expression of GFP in the transgenic mice. GFP was detected in the spleen cells, bone marrow cells, and neutrophils isolated from mice homozygous for the disrupted PI3K γ genes, but not those from wild-type mice (Fig. 1C). No GFP proteins were detected in other tested tissue samples of the PI3K γ -deficient mice. These results suggest that the expression of PI3K γ may be restricted to hematopoietic cells. GFP was detected with flow cytometry in over 90% of Mac1⁺ cells in the peritoneum, and about 82% of CD45R⁺ and 70% of CD3⁺ cells from the spleens of transgenic mice also expressed GFP (10).

Chemoattractants can also activate PLC, leading to transient increases in intracellular Ca²⁺ concentrations. PLC-deficient mouse lines were generated to investigate the roles of PLC- β isoforms in leukocyte functions (Fig. 1D) (11). *f*MLP-induced inositol trisphosphate (IP₃) production and Ca²⁺ efflux were not detected in neutrophils lacking PLC- β 2 and PLC- β 3 (PLC- β 2/ β 3), while cells lacking only PLC- β 2 also show clear reduction in IP₃ production and Ca²⁺ efflux (Fig. 1, E and F). Similar results were also observed with the other chemoattractants interleukin-8 (IL-8) and macrophage inflammatory protein (MIP)-1 α (10). All these results support the conclusion that PLC- β 2 and PLC- β 3 are the sole PLC isoforms that are activated by chemoattractants in mouse neutrophils.

Chemoattractants induce various responses in leukocytes, one of which is chemotaxis. Neutrophils purified from casein-treated PLC- β 2/ β 3-null mice did not show differences from wild-type cells in *f*MLP-induced (Fig. 2A) or IL-8-induced (10) chemotactic activities. Thus, we conclude that the PLC pathway is not required for chemotaxis in neutrophils. Consistent with our previous report (9), PLC- β 2/ β 3-null neutrophils showed enhanced chemotactic activities in response to the CC chemokine MIP-1 α (Fig. 2B). PI3K γ deficiency impaired

¹Department of Pharmacology, University of Rochester, Rochester, NY 14642, USA. ²Department of Genetics and Developmental Biology, University of Connecticut Health Center, Farmington, CT 06030, USA.

*These authors contributed equally to this work.

†Present address: Department of Pharmacology, Boehringer Ingelheim Pharmaceuticals, Inc., Ridgefield, CT 06877, USA.

‡To whom correspondence should be addressed. E-mail: dwu@neuron.uch.edu